HHS Public Access

Author manuscript

Radiology. Author manuscript; available in PMC 2015 September 22.

Published in final edited form as:

Radiology. 2015 August ; 276(2): 408–415. doi:10.1148/radiol.2015141648.

Automated Quantitative Plaque Burden from Coronary CT Angiography Noninvasively Predicts Hemodynamic Significance by Using Fractional Flow Reserve in Intermediate Coronary Lesions[1]

Mariana Diaz-Zamudio, MD, **Damini Dey, PhD**, **Annika Schuhbaeck, MD**, **Ryo Nakazato, MD, PhD**, **Heidi Gransar, PhD**, **Piotr J. Slomka, PhD**, **Jagat Narula, MD, PhD**, **Daniel S. Berman, MD**, **Stephan Achenbach, MD**, **James K. Min, MD**, **Joon-Hyung Doh, MD, PhD**, and **Bon-Kwon Koo, MD, PhD**

Department of Imaging and Medicine, Division of Nuclear Medicine (M.D.Z., R.N., H.G., P.J.S., D.S.B.), and Biomedical Imaging Research Institute (D.D.), Cedars-Sinai Medical Center, 8700 Beverly Blvd, S. Mark Taper Building A238, Los Angeles, CA 90048; Department of Internal Medicine 2, University of Erlangen, Erlangen, Germany (A.S., S.A.); Cardiovascular Institute, Mount Sinai Medical Center, New York, NY (J.N.); Department of Radiology, Weill Cornell Medical College, New York-Presbyterian Hospital, New York, NY (J.K.M.); Department of Medicine, Inje University Ilsan-Paik Hospital, Goyang, South Korea (J.H.D.); and Department of Medicine, Seoul National University Hospital, Seoul, South Korea (B.K.K.)

Abstract

Purpose—To evaluate the utility of multiple automated plaque measurements from coronary computed tomographic (CT) angiography in determining hemodynamic significance by using invasive fractional flow reserve (FFR) in patients with intermediate coronary stenosis.

[1]This research was supported by the National Institutes of Health/NHLBI (grants R01HL111141, R01HL115150, R01HL118019, and U01HL105907)and the German government, Bundesministerium für Bildung und Forschung (grant 01EX1012B).

Address correspondence to D.D. (Damini.Dey@cshs.org).

Author contributions:

Guarantors of integrity of entire study, M.D.Z., D.D., J.K.M.; study concepts/study design or data acquisition or data analysis/interpretation, all authors; manuscript drafting or manuscript revision for important intellectual content, all authors; approval of final version of submitted manuscript, all authors; agrees to ensure any questions related to the work are appropriately resolved, all authors; literature research, M.D.Z., D.D., R.N., P.S., J.N., D.S.B., J.K.M.; clinical studies, A.S., R.N., D.S.B., J.K.M., J.H.D., B.K.K.; experimental studies, D.D., R.N., P.S., J.K.M.; statistical analysis, M.D.Z., D.D., R.N., H.G., P.S., J.K.M.; and manuscript editing, M.D.Z., D.D., A.S., R.N., P.S., J.N., D.S.B., S.A., J.K.M., B.K.K.

Disclosures of Conflicts of Interest: M.D.Z. disclosed no relevant relationships. **D.D.** Activities related to the present article: none to disclose. Activities not related to the present article: received royalties for software from Cedars-Sinai Medical Center and has a patent pending. Other relationships: none to disclose. **A.S.** disclosed no relevant relationships. **R.N.** disclosed no relevant relationships. **H.G.** disclosed no relevant relationships. **P.J.S.** Activities related to the present article: none to disclose. Activities not related to the present article: receives software royalties from Cedars-Sinai Medical Center, has a patent pending. Other relationships: none to disclose. **J.N.** disclosed no relevant relationships. **D.S.B.** Activities related to the present article: none to disclose. Activities not related to the present article: received royalties for software and personal fees from Cedars-Sinai Medical Center, has a patent pending. Other relationships: none to disclose. **S.A.** Activities related to the present article: none to disclose. Activities not related to the present article: received a grant from Abbott Vascular. Other relationships: none to disclose. **J.K.M.** Activities related to the present article: none to disclose. Activities not related to the present article: member of the board of Arineta; consultant for HeartFlow, NeoGraft Technologies, MyoKardia, CardioDx, and Abbott Vascular; research agreement with GE Healthcare. Other relationships: none to disclose. **J.H.D.** disclosed no relevant relationships. **B.K.K.** disclosed no relevant relationships.

Materials and Methods—The study was approved by the institutional review board. All patients provided written informed consent. Fifty-six intermediate lesions (with 30%–69% diameter stenosis) in 56 consecutive patients (mean age, 62 years; range, 46–88 years), who subsequently underwent invasive coronary angiography with assessment of FFR (values ≤0.80 were considered hemodynamically significant) were analyzed at coronary CT angiography. Coronary CT angiography images were quantitatively analyzed with automated software to obtain the following measurements: volume and burden (plaque volume × 100 per vessel volume) of total, calcified, and noncalcified plaque; low-attenuation (<30 HU) noncalcified plaque; diameter stenosis; remodeling index; contrast attenuation difference (maximum percent difference in attenuation per unit area with respect to the proximal reference cross section); and lesion length. Logistic regression adjusted for potential confounding factors, receiver operating characteristics, and integrated discrimination improvement were used for statistical analysis.

Results—FFR was 0.80 or less in 21 (38%) of the 56 lesions. Compared with nonischemic lesions, ischemic lesions had greater diameter stenosis (65% vs 52%, $P = .02$) and total (49% vs 37%, $P = .0003$), noncalcified (44% vs 33%, $P = .0004$), and low-attenuation noncalcified (9% vs 4%, $P < .0001$) plaque burden. Calcified plaque and remodeling index were not significantly different. In multivariable analysis, only total, noncalcified, and low-attenuation noncalcified plaque burden were significant predictors of ischemia ($P < .015$). For predicting ischemia, the area under the receiver operating characteristics curve was 0.83 for total plaque burden versus 0.68 for stenosis ($P = .04$).

Conclusion—Compared with stenosis grading, automatic quantification of total, noncalcified, and low-attenuation noncalcified plaque burden substantially improves determination of lesion-specific hemodynamic significance by FFR in patients with intermediate coronary lesions.

Coronary computed tomographic (CT) angiography has proved to be a reliable and reproducible noninvasive method for the assessment of coronary artery disease (1,2). Recent studies suggest that the decision to perform revascularization should be based not only on the grade of anatomic stenosis but also on the functional significance of coronary lesions, a characteristic that is not accurately determined by the degree of stenosis. Fractional flow reserve (FFR) has become the currently accepted standard for assessment of lesion-specific ischemia, and revascularization decisions made on the basis of lesion-specific ischemia with invasive FFR have been shown to substantially reduce subsequent adverse cardiac events compared with standard invasive coronary angiography–guided revascularization (3–5). CT angiography provides the ability to assess a variety of plaque characteristics in addition to stenosis. The aim of this study was to evaluate the performance of multiple automated plaque measurements from coronary CT angiography in determining lesion-specific hemodynamic significance with invasive FFR in patients with intermediate (30%–69%) coronary stenosis.

Materials and Methods

Patients

The study was approved by the institutional review board of the study centers, and all patients provided written informed consent. From September 2006 to November 2011, we studied 56 consecutive patients with at least one isolated area of intermediate stenosis (in the

range of 30%–69%) in the proximal or mid portion of a major epicardial coronary artery that was visually identified at CT angiography in patients with clinically indicated FFR who underwent invasive coronary angiography within 3 months (3,6). Coronary CT angiography was performed because of the presence of clinically suspected coronary artery disease on the basis of symptoms and risk factors. All patients were symptomatic at the time of coronary CT angiography and diagnostic catheterization. Inclusion criteria included completion of FFR evaluation and no change in clinical characteristics, symptoms, events, or treatment regimen between CT angiography and invasive coronary angiography. The exclusion criterion for quantitative image analysis was poor coronary CT angiography image quality; no patients were excluded on the basis of this criterion.

Coronary CT Angiography

Coronary CT angiography was performed according to the guidelines of the Society of Cardiovascular Computed Tomography for performing coronary CT angiography with two imagers (dual-source [Somatom Definition; Siemens, Forchheim, Germany] or 320–detector row [Aquilion One; Toshiba, Otawara, Japan] CT) (7). All patients received nitroglycerin, and those with a heart rate over 65 beats per minute were given β blockers unless a contraindication was present. An intravenous bolus (60–90 mL) of contrast material (Omnipaque 350; GE Healthcare, Princeton, NJ, or Visipaque 320; GE Healthcare, Princeton, NJ) was injected at a flow rate of 4–6 mL/sec. For dual-source CT, the following imaging parameters were used: tube current time product of 350 mAs per rotation and tube voltage of 100 or 120 kVp. Transaxial images were reconstructed with 0.750-mm section thickness and a medium-smooth convolution kernel. For the Aquilion One scanner, tube current of 200–400 mA and tube voltage of 100 or 120 kVp were used for image acquisition, and transaxial images were reconstructed with 0.6-mm section thickness. For both scanners, either prospective or retrospective electrocardiography gating (with x-ray tube current modulation for retrospective electrocardiography-gated protocols) was used for image acquisition. Timing bolus or bolus tracking, depending on the protocol, was used. Sharp kernel reconstruction series were not deemed necessary for visual assessment of calcified plaque or stenosis. For helical images, the position of the reconstruction window within the cardiac cycle was individually selected to minimize artifacts. Motion-free data sets, typically in mid diastole, were collected for analysis. All studies were considered diagnostic image quality with optimal contrast enhancement and no substantial motion artifacts. Radiation dose (dose length product) for coronary CT angiography was 142–714 mGyμcm (8).

Invasive Coronary Angiography and Measurement of FFR

Selective invasive coronary angiography was performed by way of standard catheterization in accordance with the guidelines of the American College of Cardiology for coronary angiography (9). FFR was measured with a 0.014-inch pressure sensor–tipped guide wire (PressureWire; St Jude Medical Systems, St Paul, Minn), as was previously described (10). Hyperemia was induced with administration of an intracoronary bolus (80 μg in the left coronary artery and 40 μg in the right coronary artery) or continuous infusion (140 μg/kg per minute) of intravenous adenosine (11). Intracoronary nitroglycerin was administered immediately before measurement of FFR. An FFR value of 0.80 or more was considered

abnormal (3). Interventional cardiologists were fully blinded to the quantitative evaluation of CT angiography images.

Analysis of Coronary CT Angiography

Automated assessment of multiple plaque characteristics of the coronary lesions was performed with a previously developed automated algorithm (Autoplaq, version 9.6; Cedars-Sinai Medical Center, Los Angeles, Calif) on a standard 3.0-GHz computer workstation that runs Windows (Microsoft, Redmond, Wash) (12,13). The location where FFR was performed is directly marked on CT angiograms, and quantitative plaque characteristics were measured in segments up to this location. Stenosis measurements derived from automated analysis included the maximum diameter of stenosis and the maximum area of stenosis. The quantitative percentage of stenosis was calculated by dividing the narrowest lumen diameter by the mean of two healthy, nondiseased reference points. As was previously described, the absolute volumes for total, noncalcified, and calcified plaque were calculated by using image-specific thresholds (12,13). Low-attenuation noncalcified plaque was defined as noncalcified plaque below a preset low-attenuation threshold of 30 HU (14). The plaque burden for each category (total, noncalcified, and calcified) was calculated and defined as the plaque volume normalized to the vessel volume (plaque volume × 100%/ vessel volume). The remodeling index was determined as the ratio of maximum vessel area to that at the proximal healthy reference point (15). Lesion length (in millimeters) was the length of the diseased vessel as computed by the quantitative software. Contrast attenuation difference over the lesion was computed as follows: The luminal contrast attenuation, which is defined as the attenuation per unit area, similar to an “area gradient,” was computed over 1-mm cross sections of the arterial segment (16). The contrast attenuation difference was defined as the maximum percent difference in contrast attenuations with respect to the proximal reference cross section (the area with no disease). To quantify each lesion, coronary CT angiography images were examined by an experienced reader (M.D.Z., with more than 3 years of experience) who was blinded to invasive coronary angiography and FFR findings up to the marked FFR location at CT angiography. For each patient, quantification was performed by only one expert reader (M.D.Z.); excellent interobserver and interimage reproducibility were previously reported (13,17). Subsequent plaque quantification was automated by using image-specific adaptive thresholds. The volumes of each segment were then summed to obtain total per-vessel plaque volumes. For each artery, maximum diameter stenosis, remodeling index, and contrast attenuation difference were reported. The final result of quantification was edited if needed and approved by the experienced reader (M.D.Z.). The time for analysis was 3–5 minutes.

Statistical Analysis

Continuous variables are expressed as a mean plus or minus a standard deviation and range. Comparisons between volumes were performed by using the paired *t* test. To examine discrimination, the areas under the receiver operating characteristics curve (AUCs) were obtained and compared for quantitative CT parameters. Multivariate logistic regression was performed for variables that were significant at univariate analysis. Because established risk categories do not exist for quantitative plaque features, patient reclassification was assessed by using the integrated discrimination improvement (IDI) index (18). The IDI index was

calculated for each model. Statistical analysis was performed with STATA version 11 (StataCorp LP, College Station, Tex) and Analyze-it software (Analyze-it Software, Leeds, England). IDI analyses were performed with SAS 9.2 software (SAS Institute, Cary, NC). *P* value less than .05 was considered to indicate a statistically significant difference.

Results

Patient Characteristics

The mean patient age was 62.4 years ± 9.0 (range, 46–88). Mean ages for women and men were 60.1 years ± 8.1 and 62.9 years ± 9.1, respectively, with no significant differences (*P* = .4). Demographic and clinical characteristics are listed in Table 1. There was no difference in any characteristics between the patients in the ischemic group and those in the nonischemic group. The median time between coronary CT angiography and invasive coronary angiography was 21 days (range, 13–35 days). During this time, no change in clinical characteristics, symptoms, or events occurred. Of the 56 analyzed coronary artery lesions, 36 (64.3%) were in the left anterior descending coronary artery, 15 (26.8%) were in the right coronary artery, and five (8.9%) were in the left circumflex coronary artery. Of the intermediate stenoses, 21 (37.5%) were considered ischemic according to FFR. Figure 1 shows a case example from our study.

CT Angiography Parameters in Ischemic Versus Nonischemic Stenoses

Stenosis measurements (both the maximum diameter and the maximum area of stenosis) were significantly higher in lesions with an FFR of 0.80 or less than they were in those with an FFR above 0.80. Lesions with hemodynamic relevance had significantly higher plaque volumes (256.7 vs 173.7 cm^3, *P* = .005) and plaque burden (48.5% vs 37.2%, *P* = .0003) than did lesions that were not hemodynamically relevant according to FFR. Similarly, at a *P* < .05 level of statistical significance, the volumes and burden of noncalcified and low-attenuation noncalcified plaque were significantly higher in hemodynamic relevance (Table 2). Conversely, volume and burden of calcified plaque were not significantly different between ischemic and nonischemic lesions. Contrast attenuation difference was significantly higher in ischemic lesions (23.7 vs 18.9%, *P* = .03), whereas remodeling index and lesion length were not significantly different (Table 2).

At multivariate analysis, which was adjusted by age and sex, only total, noncalcified, and low-attenuation plaque burden were significant predictors of ischemia (Table 3). For low-attenuation noncalcified plaque, the association persisted even when noncalcified and total plaque burden were added (low-attenuation noncalcified plaque: odds ratio, 1.32; *P* = .037; total plaque: odds ratio, 1.09, *P* = .07). In contrast, the calcified plaque burden was not significant (*P* = .94) in this multivariable analysis.

Discrimination of Ischemic Lesions

Discriminative powers for independent predictors of hemodynamic relevance were compared with the use of receiver operating characteristics analysis (Fig 2). When plaque burden measurements were separately considered, the AUC for determining whether FFR was 0.80 or less was significantly higher for total plaque burden (AUC, 0.83; 95%

confidence interval [CI]: 0.71, 0.93) than for maximum diameter stenosis (AUC, 0.69; 95% CI: 0.54, 0.82; *P* = .036). The AUC for noncalcified plaque burden (AUC, 0.78; 95% CI: 0.65, 0.91; *P* = .13] and low-attenuation noncalcified plaque burden (AUC, 0.79; 95% CI: 0.65, 0.92; *P* = .19) showed a trend to being higher than did that for maximum diameter stenosis. Further, the AUC for the additive value of total plaque burden to maximum diameter stenosis was also significantly higher than that for maximum diameter stenosis alone (AUC, 0.83; 95% CI: 0.71, 0.93; *P* = .033).

The optimal threshold for the use of total plaque burden to identify hemodynamically relevant coronary artery stenoses was 42%. This threshold led to a sensitivity of 90.5% and specificity of 74.3%. For diameter stenosis determined at coronary CT angiography, the optimal threshold was greater than 50% lumen reduction, which led to a sensitivity of 90.5% and specificity of 37.1% and was significantly lower than that for plaque burden (*P* = . 0033).

Table 4 shows the IDI for predicting ischemia for characterized plaque burden. Characterization of total, noncalcified, and low-attenuation noncalcified plaque burden significantly improved the discrimination of ischemia on a perpatient basis.

Discussion

Our results show that, in patients with intermediate coronary lesions, automatic measurement of total and noncalcified plaque burden significantly improves prediction of hemodynamic significance with FFR and is the only variable that indicates hemodynamic significance with FFR and multivariable analysis. Further, compared with stenosis, specificity was significantly improved. On a per-patient basis, quantitative plaque burden significantly improved risk reclassification for predicting ischemia (total, noncalcified, and low-attenuation noncalcified plaque burden). Our results also suggest that low-attenuation plaque burden, a feature of plaque vulnerability, indicates hemodynamic significance with FFR.

The inaccuracy of stenosis for predicting lesion-specific ischemia is well known. In the FFR versus angiography for multivessel evaluation, or FAME, study, Tonino et al (19) reported that 65% of lesions that were considered to be of 50%–70% stenosis were not ischemic according to FFR. While the accuracy of coronary CT angiography for depicting anatomic coronary stenosis by way of invasive coronary angiography is high, as with invasive coronary angiography, the accuracy of stenosis at CT angiography for detecting ischemia by FFR is much lower (20). On the basis of quantification of stenosis alone, previous studies support a good correlation with stenosis grade at quantitative invasive coronary angiography and a fair but insufficient correlation with ischemia by FFR (21,22). The inaccuracy of stenosis variables for indicating ischemia may be related to plaque characteristics beyond the grade of stenosis, such as plaque length, geometry, volume, burden, and components. Because of the ability of coronary CT angiography to depict these characteristics, quantitative plaque measurement could potentially increase the performance of coronary CT angiography in differentiating among ischemic and nonischemic lesions.

Regarding plaque features, previous studies have shown that assessment of plaque characteristics could increase the performance and specificity of CT angiography for depicting ischemia (23–25). In general, our results are in accordance with these previous studies and build upon previous results by including not previously reported quantitative parameters derived from automated evaluation, particularly plaque burden, plaque composition, and contrast attenuation difference. Furthermore, to date, most of these quantitative assessments are based on manual methods that are both highly subjective and time consuming.

Several plaque characteristics may contribute to hemodynamic significance of stenosis and include anatomic factors such as plaque length and morphologic characteristics and physiologic factors such as impaired hyperemic responses arising from endothelial dysfunction and dynamic vasoconstriction. Pathophysiologically, the total atherosclerosis proximal to a coronary lesion has been demonstrated to be an important contributor to its hemodynamic status. De Bruyne et al (26) reported that early-stage coronary atherosclerosis is often associated with abnormal resistance of the coronary arteries before high-grade stenosis is apparent at angiography by way of invasive coronary angiography. Atherosclerotic coronary arteries without high-grade stenosis often manifest as a continuous pressure decline along their length, and they reduce coronary flow reserve and contribute to myocardial ischemia. A study by Naya et al (27) of the relationship of visually assessed total coronary plaque burden and composition at CT angiography with impaired regional myocardial flow reserve measured at rubidium 82 positron emission tomography suggested that noncalcified plaque may be a surrogate marker of more diffuse coronary microvascular dysfunction. A recent histopathologic investigation demonstrated that the best discriminator of vulnerable plaque is the thickness of the fibrous cap, followed by macrophage infiltration and necrotic core. Further, in those who experienced sudden cardiac death, a high proportion of culprit lesions were found to cause obstructive luminal stenosis, particularly in later stages of plaque development (28). It has been suggested that plaque vulnerability may be related to hemodynamic perturbations and altered shear stress in the coronary arteries (29,30). A previous study by Shmilovich et al (24) showed that the high-risk plaque features of lipid core and positive remodeling indicate myocardial ischemia and may be useful in assessing the hemodynamic significance of stenotic lesions. Our findings that total, noncalcified, and low-attenuation noncalcified plaque burden—prognostically important plaque measures—substantially improve determination of the hemodynamic significance of intermediate lesions, add to the studies reported thus far, and further enhance these pathophysiologic hypotheses.

Other coronary CT angiography–based methods for predicting lesion-specific ischemia have been described and include assessment of transluminal attenuation gradient and noninvasive FFR derived from coronary CT angiography and CT perfusion. FFR derived from coronary CT angiography has shown good results in determining invasive FFR (15, 31–33). Wong et al (34) reported that transluminal attenuation gradient was as accurate as CT stress perfusion in predicting ischemia by FFR. The combination of CT perfusion and coronary CT angiography showed improved diagnostic accuracy for depicting ischemia by way of invasive coronary angiography and single photon emission CT–myocardial perfusion imaging compared with CT angiography alone (35). The possibility that the quantitative

plaque features we described may be used in combination with one or more of these other methods for predicting ischemia is promising and merits further exploration.

A major limitation of this study is the relatively small sample size and the potential biases that are introduced by the selection of patients who underwent invasive coronary angiography and FFR. Because of the invasive nature and cost of FFR, it was performed only in individuals with intermediate coronary stenosis seen at invasive coronary angiography. Some patients with intermediate stenosis at CT angiography would not have been included in this study, and, in our cohort, some lesions with intermediate stenosis at CT angiography were not studied with FFR; we limited our analysis to lesions with intermediate degrees of luminal stenosis at coronary CT angiography. Whether plaque burden is also predictive of hemodynamic significance in lesions with more severe luminal stenosis was not examined.

Our findings suggest that automated measurement of plaque characteristics and, specifically, plaque burden, which is expressed as the percent of the volume of the artery that contains plaque, have the potential to help guide management of patients with intermediate coronary stenosis and can potentially be used as a tool in distinguishing hemodynamically significant lesions.

Abbreviations

AUC	area under the receiver operating characteristics curve
CI	confidence interval
FFR	fractional flow reserve
IDI	integrated discrimination improvement

References

1. Meijboom WB, Meijs MF, Schuijf JD, et al. Diagnostic accuracy of 64-slice computed tomography coronary angiography: a prospective, multicenter, multivendor study. J Am Coll Cardiol. 2008; 52(25):2135–2144. [PubMed: 19095130]
2. Budoff MJ, Dowe D, Jollis JG, et al. Diagnostic performance of 64-multidetector row coronary computed tomographic angiography for evaluation of coronary artery stenosis in individuals without known coronary artery disease: results from the prospective multicenter ACCURACY (assessment by coronary computed tomographic angiography of individuals undergoing invasive coronary angiography) trial. J Am Coll Cardiol. 2008; 52(21):1724–1732. [PubMed: 19007693]
3. Tonino PA, De Bruyne B, Pijls NH, et al. Fractional flow reserve versus angiography for guiding percutaneous coronary intervention. N Engl J Med. 2009; 360(3):213–224. [PubMed: 19144937]
4. Nam CW, Yoon HJ, Cho YK, et al. Outcomes of percutaneous coronary intervention in intermediate coronary artery disease: fractional flow reserve–guided versus intravascular ultrasound–guided. JACC Cardiovasc Interv. 2010; 3(8):812–817. [PubMed: 20723852]
5. Pijls NH, Fearon WF, Tonino PA, et al. Fractional flow reserve versus angiography for guiding percutaneous coronary intervention in patients with multivessel coronary artery disease: 2-year follow-up of the FAME (fractional flow reserve versus angiography for multivessel evaluation) study. J Am Coll Cardiol. 2010; 56(3):177–184. [PubMed: 20537493]

6. Nakazato R, Park HB, Berman DS, et al. Noninvasive fractional flow reserve derived from computed tomography angiography for coronary lesions of intermediate stenosis severity: results from the DeFACTO study. Circ Cardiovasc Imaging. 2013; 6(6):881–889. [PubMed: 24081777]
7. Abbara S, Arbab-Zadeh A, Callister TQ, et al. SCCT guidelines for performance of coronary computed tomographic angiography: a report of the Society of Cardiovascular Computed Tomography Guidelines Committee. J Cardiovasc Comput Tomogr. 2009; 3(3):190–204. [PubMed: 19409872]
8. Halliburton SS, Abbara S, Chen MY, et al. SCCT guidelines on radiation dose and dose-optimization strategies in cardiovascular CT. J Cardiovasc Comput Tomogr. 2011; 5(4):198–224. [PubMed: 21723512]
9. Scanlon PJ, Faxon DP, Audet AM, et al. ACC/AHA guidelines for coronary angiography: a report of the American College of Cardiology/American Heart Association Task Force on practice guidelines (Committee on Coronary Angiography)—developed in collaboration with the Society for Cardiac Angiography and Interventions. J Am Coll Cardiol. 1999; 33(6):1756–1824. [PubMed: 10334456]
10. MacCarthy P, Berger A, Manoharan G, et al. Pressure-derived measurement of coronary flow reserve. J Am Coll Cardiol. 2005; 45(2):216–220. [PubMed: 15653018]
11. De Bruyne B, Pijls NH, Barbato E, et al. Intracoronary and intravenous adenosine 5′-triphosphate, adenosine, papaverine, and contrast medium to assess fractional flow reserve in humans. Circulation. 2003; 107(14):1877–1883. [PubMed: 12668522]
12. Dey D, Schepis T, Marwan M, Slomka PJ, Berman DS, Achenbach S. Automated three-dimensional quantification of noncalcified coronary plaque from coronary CT angiography: comparison with intravascular US. Radiology. 2010; 257(2):516–522. [PubMed: 20829536]
13. Dey D, Cheng VY, Slomka PJ, et al. Automated 3-dimensional quantification of noncalcified and calcified coronary plaque from coronary CT angiography. J Cardiovasc Comput Tomogr. 2009; 3(6):372–382. [PubMed: 20083056]
14. Motoyama S, Sarai M, Harigaya H, et al. Computed tomographic angiography characteristics of atherosclerotic plaques subsequently resulting in acute coronary syndrome. J Am Coll Cardiol. 2009; 54(1):49–57. [PubMed: 19555840]
15. Achenbach S, Ropers D, Hoffmann U, et al. Assessment of coronary remodeling in stenotic and nonstenotic coronary atherosclerotic lesions by multidetector spiral computed tomography. J Am Coll Cardiol. 2004; 43(5):842–847. [PubMed: 14998627]
16. Steigner ML, Mitsouras D, Whitmore AG, et al. Iodinated contrast opacification gradients in normal coronary arteries imaged with prospectively ECG-gated single heart beat 320–detector row computed tomography. Circ Cardiovasc Imaging. 2010; 3(2):179–186. [PubMed: 20044512]
17. Schuhbaeck A, Dey D, Otaki Y, et al. Interscan reproducibility of quantitative coronary plaque volume and composition from CT coronary angiography using an automated method. Eur Radiol. 2014; 24(9):2300–2308. [PubMed: 24962824]
18. Pencina MJ, D'Agostino RB, Pencina KM, Janssens AC, Greenland P. Interpreting incremental value of markers added to risk prediction models. Am J Epidemiol. 2012; 176(6):473–481. [PubMed: 22875755]
19. Tonino PA, Fearon WF, De Bruyne B, et al. Angiographic versus functional severity of coronary artery stenoses in the FAME study fractional flow reserve versus angiography in multivessel evaluation. J Am Coll Cardiol. 2010; 55(25):2816–2821. [PubMed: 20579537]
20. Nørgaard BL, Leipsic J, Gaur S, et al. Diagnostic performance of noninvasive fractional flow reserve derived from coronary computed tomography angiography in suspected coronary artery disease: the NXT trial (analysis of coronary blood flow using CT angiography: next steps). J Am Coll Cardiol. 2014; 63(12):1145–1155. [PubMed: 24486266]
21. Kristensen TS, Engstrøm T, Kelbæk H, von der Recke P, Nielsen MB, Kofoed KF. Correlation between coronary computed tomographic angiography and fractional flow reserve. Int J Cardiol. 2010; 144(2):200–205. [PubMed: 19427706]
22. Voros S, Rinehart S, Vazquez-Figueroa JG, et al. Prospective, head-to-head comparison of quantitative coronary angiography, quantitative computed tomography angiography, and intravascular ultrasound for the prediction of hemodynamic significance in intermediate and

severe lesions, using fractional flow reserve as reference standard (from the ATLANTA I and II study). Am J Cardiol. 2014; 113(1):23–29. [PubMed: 24238960]

23. Nakazato R, Shalev A, Doh JH, et al. Aggregate plaque volume by coronary computed tomography angiography is superior and incremental to luminal narrowing for diagnosis of ischemic lesions of intermediate stenosis severity. J Am Coll Cardiol. 2013; 62(5):460–467. [PubMed: 23727206]
24. Shmilovich H, Cheng VY, Tamarappoo BK, et al. Vulnerable plaque features on coronary CT angiography as markers of inducible regional myocardial hypoperfusion from severe coronary artery stenoses. Atherosclerosis. 2011; 219(2):588–595. [PubMed: 21862017]
25. Rossi A, Papadopoulou SL, Pugliese F, et al. Quantitative computed tomographic coronary angiography: does it predict functionally significant coronary stenoses? Circ Cardiovasc Imaging. 2014; 7(1):43–51. [PubMed: 24280729]
26. De Bruyne B, Hersbach F, Pijls NHJ, et al. Abnormal epicardial coronary resistance in patients with diffuse atherosclerosis but “normal” coronary angiography. Circulation. 2001; 104(20):2401–2406. [PubMed: 11705815]
27. Naya M, Murthy VL, Blankstein R, et al. Quantitative relationship between the extent and morphology of coronary atherosclerotic plaque and downstream myocardial perfusion. J Am Coll Cardiol. 2011; 58(17):1807–1816. [PubMed: 21996395]
28. Narula J, Nakano M, Virmani R, et al. Histopathologic characteristics of atherosclerotic coronary disease and implications of the findings for the invasive and noninvasive detection of vulnerable plaques. J Am Coll Cardiol. 2013; 61(10):1041–1051. [PubMed: 23473409]
29. Fearon WF. Is a myocardial infarction more likely to result from a mild coronary lesion or an ischemia-producing one? Circ Cardiovasc Interv. 2011; 4(6):539–541. [PubMed: 22186104]
30. Maurovich-Horvat P, Ferencik M, Voros S, Merkely B, Hoffmann U. Comprehensive plaque assessment by coronary CT angiography. Nat Rev Cardiol. 2014; 11(7):390–402. [PubMed: 24755916]
31. Berman DS, Stoebner RA, Dey D. Combined anatomy and physiology on coronary computed tomography angiography: a step or two in the right direction. J Am Coll Cardiol. 2014; 63(18): 1913–1915. [PubMed: 24657698]
32. Wong DT, Ko BS, Cameron JD, et al. Transluminal attenuation gradient in coronary computed tomography angiography is a novel noninvasive approach to the identification of functionally significant coronary artery stenosis: a comparison with fractional flow reserve. J Am Coll Cardiol. 2013; 61(12):1271–1279. [PubMed: 23414792]
33. Taylor CA, Fonte TA, Min JK. Computational fluid dynamics applied to cardiac computed tomography for noninvasive quantification of fractional flow reserve: scientific basis. J Am Coll Cardiol. 2013; 61(22):2233–2241. [PubMed: 23562923]
34. Wong DT, Ko BS, Cameron JD. Comparison of diagnostic accuracy of combined assessment using adenosine stress computed tomography perfusion + computed tomography angiography with transluminal attenuation gradient + computed tomography angiography against invasive fractional flow reserve. J Am Coll Cardiol. 2014; 63(18):1904–1912. [PubMed: 24657696]
35. George RT, Arbab-Zadeh A, Cerci RJ, et al. Diagnostic performance of combined noninvasive coronary angiography and myocardial perfusion imaging using 320-MDCT: the CT angiography and perfusion methods of the CORE320 multicenter multinational diagnostic study. AJR Am J Roentgenol. 2011; 197(4):829–837. [PubMed: 21940569]

Advances in Knowledge

- In patients with intermediate coronary lesions, automatic measurement of total plaque burden substantially improves identification of hemodynamic significance with fractional flow reserve (FFR) over stenosis (area under the receiver operator characteristic curve 0.83 vs 0.68, $P = .04$).
- Specificity for identifying hemodynamic significance on the basis of FFR is significantly improved with the use of total plaque burden compared with stenosis (74.3% vs 37.1%, $P = .0033$) in patients with intermediate lesions.

Implication for Patient Care

- Automatic measurement of plaque characteristics has the potential to help guide treatment of patients with intermediate coronary stenosis who undergo coronary CT angiography and can potentially be used as a tool to noninvasively distinguish hemodynamically significant lesions.

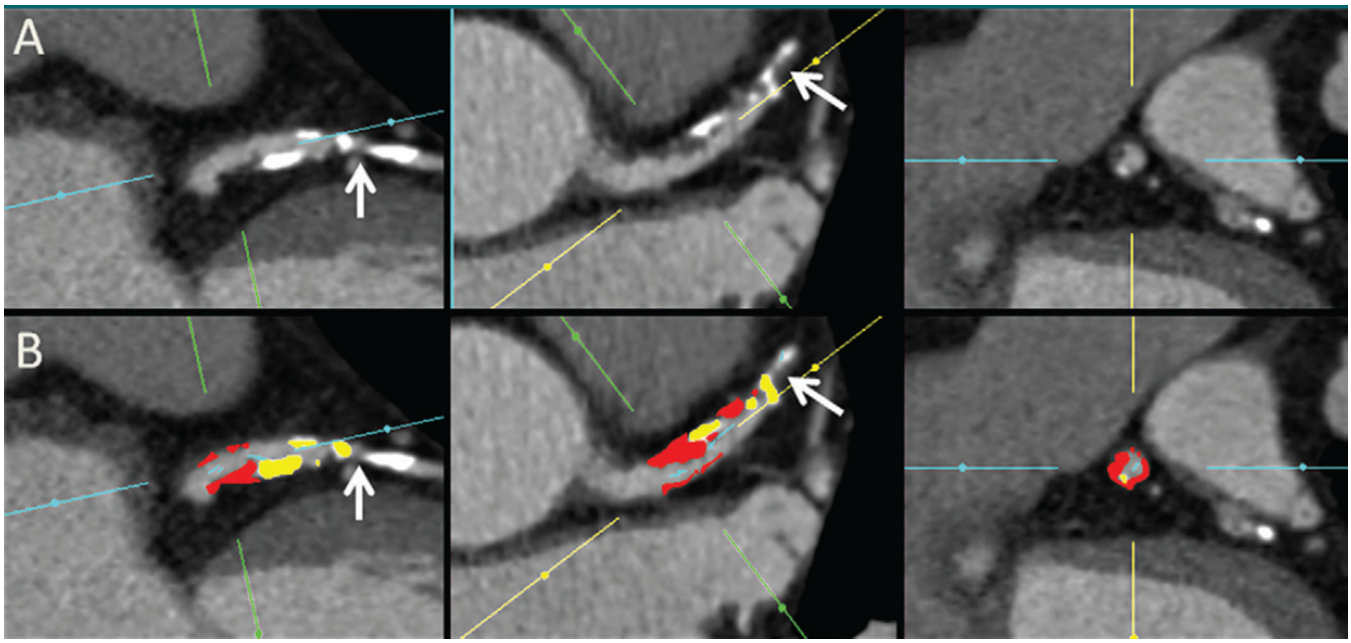

Figure 1.

Automated plaque quantification in a 65-year-old man. *A*, Long- and transverse-axis and, *B*, subsequent fully automated quantification CT angiograms obtained after manual setting of proximal and distal limits of the lesion show noncalcified (red areas), calcified (yellow areas), and low-attenuation (orange areas) plaque and the location where FFR (0.78) was performed (arrows). Despite the presence of a low-diameter stenosis (34%) and a high total (43.2%) and noncalcified (30%) plaque burden, ischemia was correctly predicted with FFR.

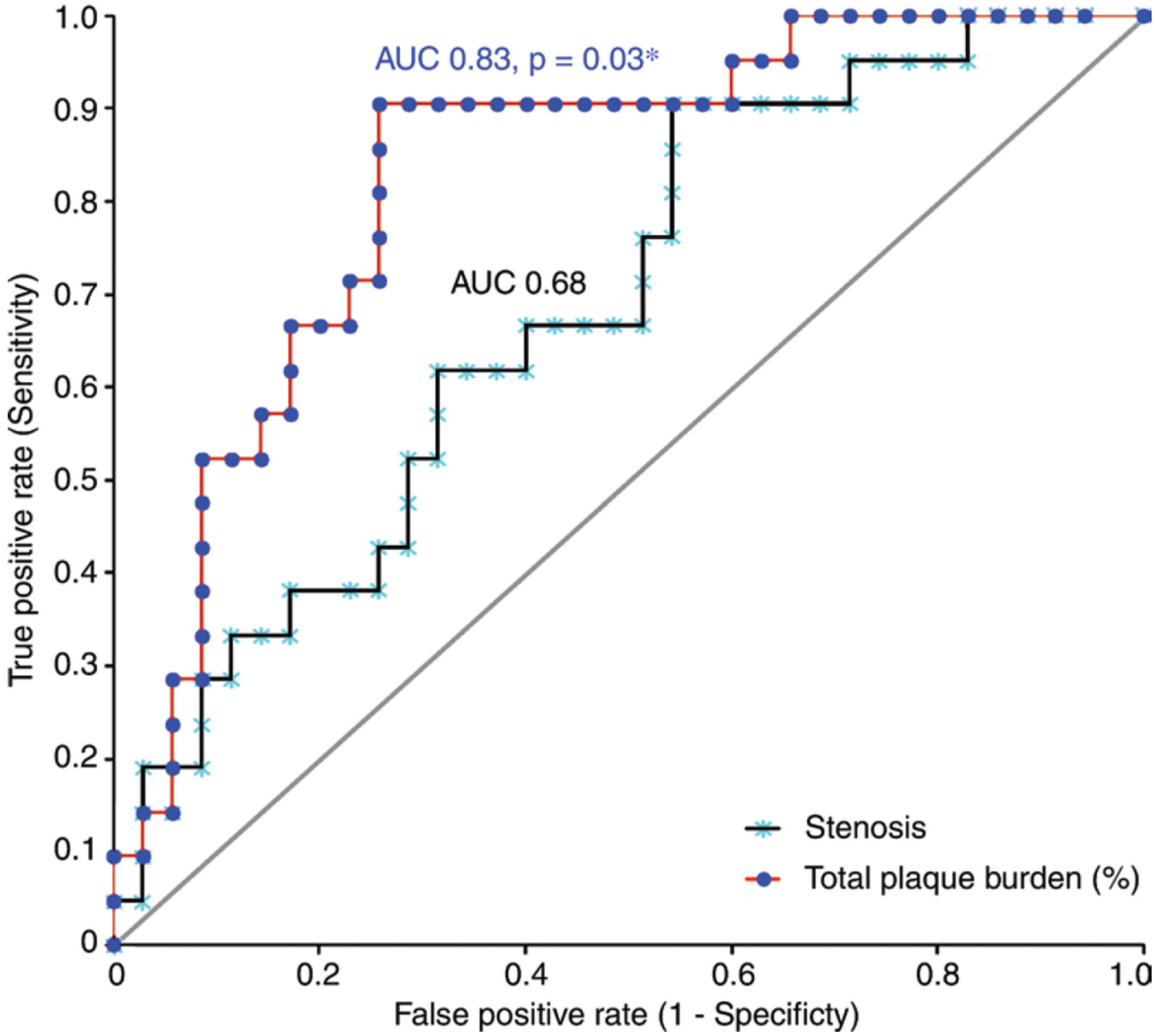

Figure 2.
Scatter plot shows AUC comparison between the total plaque burden and the maximum diameter stenosis.

Table 1

Demographic and Clinical Characteristics

Characteristic	All Patients (*n* = 56)	Nonischemic Group (*n* = 35)	Ischemic Group (*n* = 21)	*P* Value
Physical characteristics				
FFR*	0.81 ± 0.1	0.87 ± 0.04	0.71 ± 0.08	<.0001
Age (y)*	62.4 ± 9	62 ± 9	63 ± 9.1	.66
Male sex	43 (76.8)	29 (82.8)	14 (66.6)	.24
Height (cm)*	164.2 ± 7.2	165.2 ± 6.7	162.5 ± 8	.19
Weight (kg)*	67.3 ± 10	67 ± 7.8	67.9 ± 13.1	.75
BMI*	24.8 ± 2.3	24.5 ± 1.5	25.5 ± 3.3	.11
Clinical characteristics				
Diabetes	11 (19.6)	8 (22.8)	3 (14.2)	.51
Hypertension	36 (64.3)	23 (65.7)	13 (61.9)	.78
Dyslipidemia	49 (87.5)	32 (91.4)	17 (80.9)	.4
Current smoker	20 (35.7)	15 (42.8)	5 (23.8)	.24
Total cholesterol*	171.8 ± 40.7	172.1 ± 38.3	171.4 ± 45.3	.95
LDL cholesterol*	105.6 ± 33.6	105.8 ± 34.3	105.4 ± 33.2	.95
Triglycerides*	147.7 ± 73.3	157.3 ± 61.8	131.7 ± 88.7	.2
Treatment regimen				
Statin	52 (92.8)	32 (91.4)	20 (95.2)	>.99
Aspirin	52 (92.8)	31 (88.5)	21 (100)	.28
Beta blocker	19 (33.9)	11 (31.4)	8 (38)	.77
Calcium channel blocker	23 (41.1)	17 (48.6)	6 (28.5)	.14
ACE inhibitor	27 (48.2)	15 (42.8)	12 (57.1)	.4

Note.—Unless otherwise indicated, data are numbers of patients, and data in parentheses are percentages. BMI = body mass index, LDL cholesterol = low-attenuation lipoprotein cholesterol, ACE inhibitor = angiotensin-converting-enzyme inhibitor.

* Data are means plus or minus standard deviation.

Table 2

Quantitative Plaque Features in Ischemic and Nonischemic Stenoses

	Stenoses*		
Plaque Feature	**Nonischemic (*n* = 35)**	**Ischemic (*n* = 21)**	***P* Value**
Maximum diameter stenosis	52.17 ± 20.9	65 ± 13.9	.02
Maximum area stenosis	73.7 ± 24.7	86.8 ± 9.44	.02
Total plaque volume	173.7 ± 107	256.7 ± 93	.005
Noncalcified plaque volume	155.35 ± 96.6	229.3 ± 72.2	.004
Low-attenuation plaque volume	19 ± 14.8	44.5 ± 29.2	.0001
Calcified plaque volume	17.37 ± 31.7	27.34 ± 40.4	.3
Total plaque burden	37.2 ± 12.1	48.5 ± 7.2	.0003
Noncalcified plaque burden	33.4 ± 11.2	44.2 ± 8.5	.0004
Low-attenuation plaque burden	4.2 ± 2.5	8.6 ± 4.4	<.0001
Calcified plaque burden	3.6 ± 5.4	4.3 ± 5.7	.61
Remodeling index	1.49 ± 0.19	1.56 ± 1.8	.8
Contrast attenuation difference	18.9 ± 8.6	23.7 ± 9	.03
Lesion length	34.7 ± 17.2	40.2 ± 32.7	.24

*Data are means plus or minus standard deviation.

Table 3

Multivariate Analysis of Quantitative Plaque Characteristics for Lesion-Specific Ischemia

Plaque Characteristic	Odds Ratio	*P* Value
Total plaque burden	1.15 (1.04, 1.27)	.007
Noncalcified plaque burden	1.12 (1.02, 1.23)	.01
Low-attenuation plaque burden	1.43 (1.13, 1.81)	.003
Maximum diameter stenosis	1.01 (0.95, 1.05)	.95
Maximum area stenosis	1.01 (0.95, 1.07)	.59
Contrast attenuation difference	1.06 (0.96, 1.17)	.19
Lesion length	1.02 (0.98, 1.07)	.25

Note.—Data in parentheses are CIs.

Table 4

IDI for Total, Noncalcified, and Low-attenuation Noncalcified Plaque Burdens over Stenosis

Plaque Burden	IDI	95% CI	*P* Value
Total	0.17	0.06, 0.28	.002
Noncalcified	0.14	0.03, 0.25	.009
Low-attenuation noncalcified	0.20	0.05, 0.34	.006